1238 *J. Phys. Chem. A* **2001,** *105,* 1238−1243

Ultrafast Energy Equilibration in Hydrogen-Bonded Liquids

A. J. Lock,* S. Woutersen, and H. J. Bakker

FOM Institute for Atomic and Molecular Physics, Kruislaan 407, 1098 SJ Amsterdam, The Netherlands

Received: August 31, 2000; In Final Form: November 8, 2000

We have studied the equilibration dynamics of liquid water and alcohols following a local deposition of energy using time-resolved femtosecond mid-infrared pump−probe spectroscopy. The equilibration dynamics is monitored via the spectral response of the OH-stretch vibration. It is found that the equilibration leads to complicated changes of the absorption band of the OH-stretch vibration including a shift of the absorption band and a decrease of the absorption cross section. Interestingly, these spectral changes do not occur simultaneously, which indicates that they are associated with the equilibration dynamics of different low-frequency modes. For water, we find an equilibration time constant of 0.55 ± 0.05 ps. We observe that the equilibration time strongly increases going from water to alcohols such as methanol, ethanol, and propanol which means that water molecules can adapt much faster to a local deposition of energy than other hydrogen-bonding liquids.

I. Introduction

Water is the most commonly used solvent for (bio)chemical reactions. By a rearrangement of the water molecules in the surroundings of the reactive intermediates, water is able to stabilize these intermediates and to lower the energy barrier for the reaction. The dynamics of chemical reactions in aqueous solution will be governed both by the dynamics of the solvation interactions and the rate at which water molecules can accept the energy dissipated in the reaction. The solvation dynamics of water has been investigated by probing the response of solvating water molecules to an electronic rearrangement in a dissolved dye molecule.[1,2] The solvation dynamics were observed to consist of a fast inertial component with a time response of ∼50 fs and two slower, diffusive components with subpicosecond response times.

Several theoretical studies have been performed on the role of liquid water as a solvent for different solutes, ranging from peptides and biomolecules[5,6] to organic molecules[7] and HDO.[8] In ref 6, a combined quantum mechanical and classical mechanical (QM/MM) method is used. The active part of the system, for example an excited state, is treated quantum-mechanically, while the environment can be treated with molecular dynamics simulations. With this technique normal modes, potential energy surfaces, and solvent-induced spectral shifts can be obtained. The importance of water as a solvent is also illustrated in ref 7 where the relaxation of vibrationally excited CH_3Cl molecules in water is studied. It was shown that a large number of water molecules participate in the redistribution of the vibrational energy. In ref 8, molecular dynamics simulations were used to investigate the rate and mechanism of the vibrational relaxation of HDO molecules dissolved in D_2O. In this study the OH-stretch vibration was found to relax to the first overtone of the bending mode with a time constant of 7.5 ps. The excess energy of the bending mode will be accepted by the so-called bath modes, which are the low-frequency modes, such as rotations and translations of all molecules, but no time scale was given for this process of equilibration.

The outcome of molecular dynamics simulations on liquid water strongly depends on the modeling of the interactions between the water molecules.[9] Hence, there is a strong need for experimental information. In particular, one would like to know the time scale on which low-frequency water modes, such as librations and hydrogen-bond translations, respond to a local deposition of energy induced by a (bio)chemical reaction. In this respect, linear spectroscopic studies are not very informative due to the large inhomogeneity of aqueous systems. Therefore, nonlinear spectroscopic techniques using intense ultrashort pulses should be employed. Unfortunately, it is difficult to probe the response of low-frequency water modes directly on an ultrashort time scale. A solution to this problem is to follow a higher-frequency mode that is strongly coupled to these modes. For the case of the hydrogen bond, the OH-stretch vibration (ν_{OH}) forms a suitable probe, because the frequency of the OH-stretch vibration depends linearly on the hydrogen-bond length.[3,4] Hence, this vibration can be used as a probe for low-frequency hydrogen-bond dynamics that in turn represent changes in orientation and position of the water molecules.

Until now not much is known about the time scale on which water molecules react to an ultrafast dissipation of energy. Vodopyanov performed saturation studies in which water and ethanol layers were excited with intense picosecond laser radiation.[10−13] In these studies a blue shift of the OH-stretch absorption band was observed due to a rise in temperature after irradiation. From the intensity dependence of the saturation, the vibrational lifetime T_1 of the OH-stretch vibration of HDO dissolved in D_2O was estimated to be between 0.3 and 0.6 ps and the lifetime of the OH-stretch vibrations of pure H_2O was estimated to be <3 ps.[13] A major problem in these studies was that it was not possible to separate the time scale of the relaxation of the OH-stretch excitation from that of the full equilibration of the energy in the liquid. If the OH-stretch vibration relaxes to some nonthermal intermediate state, these time scales will be different. Recently, the vibrational lifetime T_1 of the OH-stretch vibration of HDO dissolved in D_2O was

---

* Author to whom correspondence should be addressed. Fax: +31-20-6684106. E-mail: a.lock@amolf.nl.

10.1021/jp003158e CCC: $20.00

measured using femtosecond mid-infrared pulses and was found to have a value of 740 fs at room temperature.[14] Since the system studied was a dilute solution of HDO, the temperature increase of the sample due to the relaxation was negligibly small and no information on the equilibration dynamics of the water was obtained.

Here we present a study on the equilibration dynamics of water and alcohols at room temperature following a local dissipation of energy. The equilibration dynamics are monitored by probing the spectral changes of the OH-stretch absorption band with femtosecond mid-infrared laser pulses. It is found that the equilibration dynamics in water are exceptionally fast in comparison to the alcohols.

II. Experimental Section

We use a Ti:Sapphire-based laser system that delivers 800 nm, 1 mJ pulses at a repetition rate of 1 kHz and a duration of about 110 fs. To get mid-infrared pulses resonant with the OH-stretch vibrational modes of liquid water, these pulses are used in an optical parametrical amplification and generation (OPA/OPG) stage based on β-BaB$_2$O$_4$. Part of the pump light is converted into signal and idler pulses with a central wavelength for the signal of 1.1 μm. A beam splitter divides the signal pulses into two parts. The strongest part of the signal is used, together with the remaining 800 nm pump light, in a second parametric amplification process in a KTiOPO$_4$ crystal to generate pulses near 3 μm.[15] The pulses can be tuned from 2.8 to 3.3 μm (3000−3600 cm^{-1}) by changing the angle of the KTP crystal, have typical energies of 15 μJ, a fwhm duration of 250 fs, and a spectral width of 80 cm^{-1}. The infrared pulses generated as described above (pump pulses) are focused on the sample and are used to excite a fraction of the molecules from the vibrational ground state to the $\nu_{OH} = 1$ state. Thereby energy is put into a specific degree of freedom.

By the same generation mechanism the second weaker part of the signal is converted to pulses around 3 μm. These pulses have the same duration and spectral width as the pump pulses and an energy per pulse of less than 1 μJ. They are also focused on the sample and are used to monitor the thermalization of the excitation of the pump pulse. The transmission of the probe and pump pulses through a 200 μm pinhole was typically 50%.

The transmission of the probe pulse with (T) and without (T_0) pump pulse are measured as a function of delay time between pump and probe pulse and the relative transmission change $\ln(T/T_0)$ is calculated. The probe polarization was set at the magic angle with respect to the polarization of the pump pulse by means of a zero-order $\lambda/2$ plate. In this way any influences of orientational relaxation on the signals[16] are ruled out.

We investigated the equilibration dynamics of pure water, methanol, ethanol, and 1-propanol. The samples consisted of a thin layer of liquid (∼1 μm for water) between two sapphire windows. To avoid heating in the sample due to former excitation pulses, the sample was rotated. The temperature rise due to a single pump pulse is calculated to be approximately 25 K for water.

III. Results

The conventional infrared absorption spectrum of water is measured with an infrared spectrometer and is depicted in Figure 1. The absorption band has its maximum at 3410 cm^{-1} and has a width of 420 cm^{-1}. It consists of two subbands stemming from the symmetric and asymmetric stretching normal modes. In Figure 2, the transmission change $\ln(T/T_0)$ as a function of delay time is shown for pure water. The molecules are excited with a pump pulse with a central frequency of $\nu = 3410$ cm^{-1} and are probed at four different frequencies. The upper curve (probe at 3500 cm^{-1}) shows a bleaching signal around $t = 0$ that with increasing delay rapidly decays and rises again to a high final level of transmission. This level of transmission

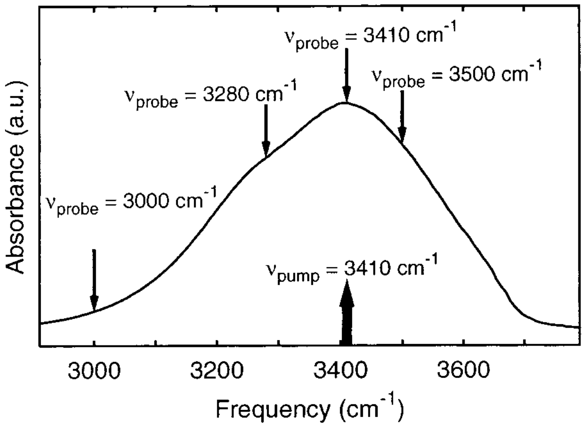

Figure 1. Absorption spectrum of the OH-stretch vibration of water at room temperature. The arrows indicate the pump and probe frequencies used in the time-resolved experiments.

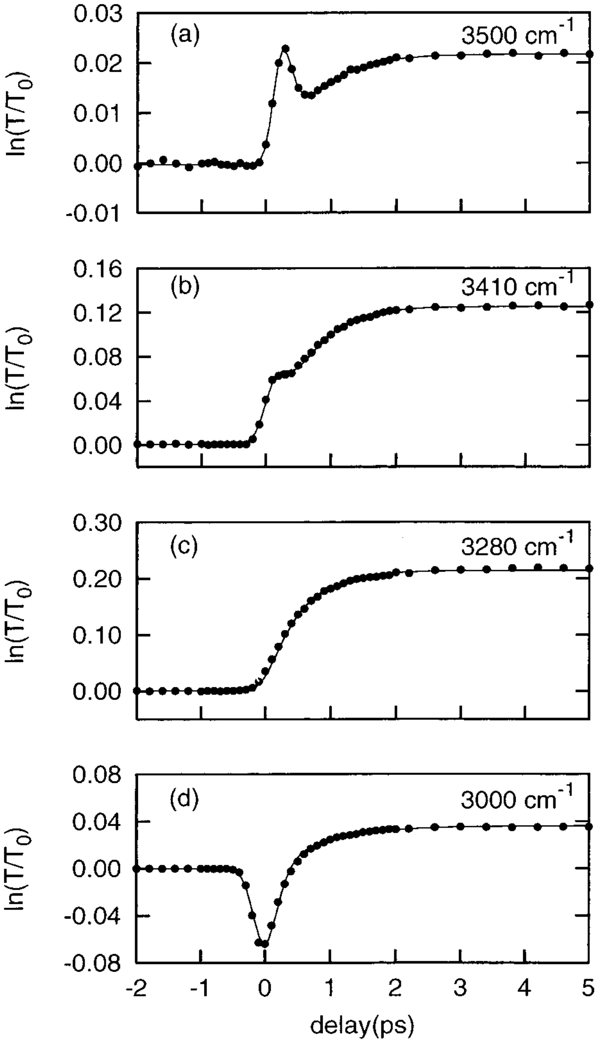

Figure 2. Transmission change $\ln(T/T_0)$ for water as a function of delay time between pump and probe pulses. The pump has a central frequency of 3410 cm^{-1}. The probe pulse has a frequency of (a) 3500 cm^{-1}, (b) 3410 cm^{-1}, (c) 3280 cm^{-1}, and (d) 3000 cm^{-1}.

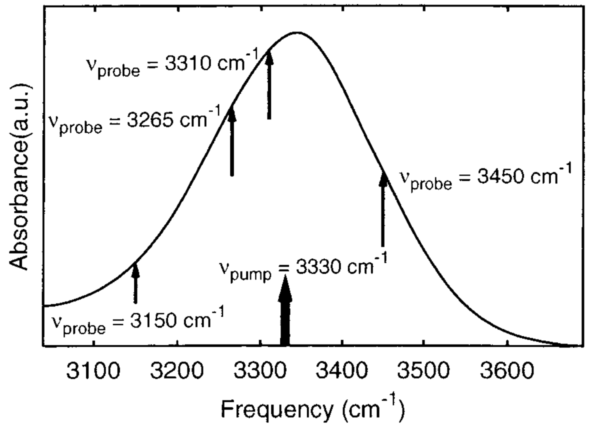

Figure 3. Absorption spectrum of the OH-stretch vibration of pure ethanol. The maximum of the band is at 3330 cm^{-1}. The pump and probe frequencies are indicated with arrows.

remains constant on a very long time scale, which indicates that this level of transmission results from the complete thermalization of the system.

When probing at the center and at the red side of the absorption band, at 3410 cm^{-1} and 3280 cm^{-1}, respectively (Figure 2b and 2c), the bleaching peak around $t = 0$ is less pronounced than at the blue side. Two reasons can be advanced for the relative peak decrease. First, with the probe frequency at the red side, we not only probe the $\nu_{OH} = 0 \rightarrow 1$ bleaching, but also the transient $\nu_{OH} = 1 \rightarrow 2$ absorption that is red-shifted by 270 cm^{-1} with respect to the $\nu_{OH} = 0 \rightarrow 1$ transition.[17] Second, at the center and at the red side of the absorption band, the long time transmission increase due to thermalization is very large and dominates the bleaching around $t = 0$. In the case that the probe wavelength equals the pump wavelength, there can be a coherent artifact[18] on the measured signal around delay zero. However, for pump and probe near 3410 cm^{-1} the influence of the coherent artifact can be neglected: at this frequency the long time transmission increase strongly dominates the bleaching already around $t = 0$. In Figure 2d the probe wavelength is tuned so far to the red edge of the absorption band that we only observe an induced $\nu_{OH} = 1 \rightarrow 2$ absorption around $t = 0$. At long delay times an increased final level of transmission is observed.

We compared the measured signals for water with results obtained for methanol, ethanol, and 1-propanol for which the hydrogen-bond strength is similar to that of water. In Figure 3, the OH-stretch absorption spectrum of pure ethanol (C_2H_5OH) is presented. The absorption spectra of methanol (CH_3OH) and 1-propanol (C_3H_7OH) are very similar to that of ethanol. Again we pump at the center frequency of the band, which is at 3330 cm^{-1} for these three alcohols. The frequencies of the probe pulses (3150, 3265, 3310, and 3450 cm^{-1}) are indicated by arrows in Figure 3.

Figure 4 shows delay time scans for pure ethanol. For Figure 4b and 4c, the observed relaxation behavior is very similar to that of water. After a bleaching at $t = 0$ and a decay at short delay times, we again observe a rise toward a permanent bleaching signal. Clearly, the same process of equilibration is observed as in water, but the time scale is dramatically different. In Figure 4d, the probe wavelength is in the red wing of the absorption band. We observe an induced $\nu_{OH} = 1 \rightarrow 2$ absorption, followed by a rise to an increased level of transmission, as was observed for water in Figure 2d. In Figure 4a, where the probe wavelength is in the blue wing of the OH-stretch absorption band, the observed signal decreases to a negative final value.

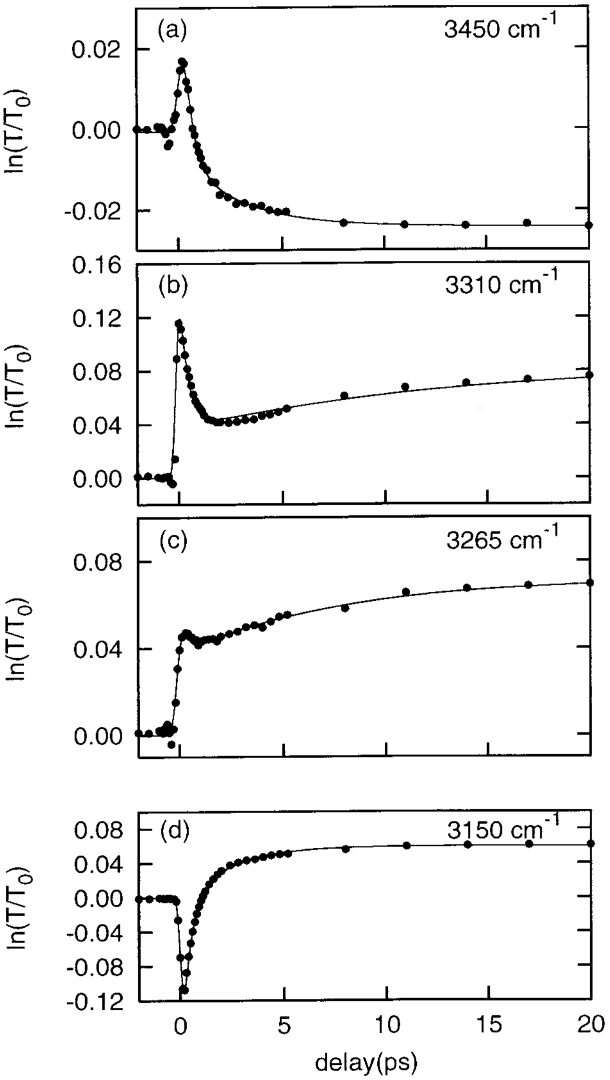

Figure 4. Delay time scans for pure ethanol after excitation with a 3330 cm^{-1} pump pulse. Transmission changes were recorded with probe pulses at the blue (a) 3450 cm^{-1}, center (b) 3310 cm^{-1}, and (c) 3265 cm^{-1} and at the red (d) 3150 cm^{-1} of the absorption band.

IV. Kinetic Modeling

The results can be interpreted in the following way. The pump pulse excites molecules from the $\nu_{OH} = 0$ to the $\nu_{OH} = 1$ state. This excited population relaxes with a time constant T_1 to an intermediate level, which is the vibrational (OH-)ground state combined with (an)other vibrational mode(s). These other vibrational modes are the HOH bending mode[19,20] and the O−H···O hydrogen bond.[21] It should be noted that the intermediate level does not yet represent thermal equilibrium, only very specific combination tones get directly excited by the relaxation of the OH-stretch vibration.

The relaxation of the intermediate level leads to a full thermalization, i.e., a redistribution of the energy over all degrees of freedom. This thermalization occurs with a time constant τ_{eq}. After equilibration, the temperature of the sample is increased which leads to longer and weaker hydrogen bonds and therefore to a blue shift of the OH-stretch resonance frequency.[3,4] As a result, the transmission at the center frequency and at the red side is strongly increased at longer delay times while at the blue side of the OH-absorption band an induced absorption is observed (Figure 4a). We do not observe an induced absorption for liquid water in Figure 2a, which is due to the fact that the increase in temperature not only leads to a blue shift of the

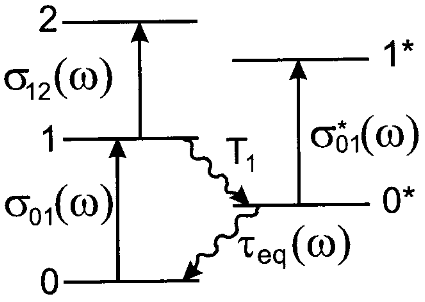

Figure 5. Energy level scheme used for fitting the data.

absorption band but also to a decrease in absorption cross-section. At the used probe frequency of 3500 cm^{-1}, the effect of the change in cross section is stronger than the effect of the blue shift.

We observe two relaxation time scales in our measurements: first, the relaxation of the excited $\nu = 1$ state of the OH-stretch vibration leading to a decay of the bleaching peak or induced absorption peak around $t = 0$ and second, the slower thermalization process that leads to an increase or decrease to a final level of transmission that remains constant on the picosecond time scale of the experiment. By changing the pump intensity we found that the thermalization (equilibration) time does not depend on the amount of energy to be equilibrated.

To fit the data we use a model depicted in Figure 5 and fully described in ref 21. It consists of the vibrational ground state (0), the first excited state (1), populated by the pump pulse, the second excited state (2), and the intermediate level 0* to which the population of state 1 relaxes with a time constant T_1. In this model, the decay of the intermediate 0*-state leads to a full thermalization of the system. The associated time scale τ_{eq} represents the equilibration or thermalization time. The absorption cross sections for the 0 → 1 and 0* → 1* transitions are $\sigma_{01}(\omega)$ and $\sigma^*_{01}(\omega)$, respectively.

The absorption of a probe beam by the sample can be denoted as follows:

$$\alpha(\omega) \propto \sigma_{01}(\omega)(n_0 - n_1) + \sigma^*_{01}(\omega)(n^*_0 - n^*_1) \tag{1}$$

where n_i denotes the population of state i. We can set $n^*_1(t) = 0$ because there is no thermal population of 0* and excitation by the probe beam will be negligible. When we substitute $n_0 = N - n_1 - n^*_0$, with N the total number of molecules and subtract the absorption of the probe without excitation by the pump pulse ($\alpha \propto \sigma N$), we get for the absorption change

$$-\Delta\alpha_{01}(\omega,t) \propto \sigma_{01}(\omega)\left(2n_1(t) + \left(1 - \frac{\sigma^*_{01}(\omega)}{\sigma_{01}(\omega)}\right)n^*_0(t)\right) + N\,\delta\sigma_{01}(\omega,t) \tag{2}$$

The $\delta\sigma_{01}(\omega)$ in the last term of eq 2 represents the change in cross section due to the temperature increase that results after the thermalization. Depending on the probe frequency this change will be positive (at the blue side of the absorption band) or negative (at the red side of the absorption band). Because the cross section change is proportional to the number of molecules relaxed from 0*, the last term can be written as

$$N\,\delta\sigma_{01}(\omega,t) \propto \int_{-\infty}^{t} \frac{n^*_0(t')}{\tau_{eq}}\,dt' \tag{3}$$

If the probe pulse only probes the 1 → 2 transition, the absorption change reads as follows:

$$\Delta\alpha_{12}(\omega,t) \propto \sigma_{12}(\omega)n_1(t) + N\,\delta\sigma_{01}(\omega,t) \tag{4}$$

We have neglected $n_2(t)$ in the above equation, which is a good approximation since the excitation fraction of $\nu_{OH} = 1$ is only about 1%. The last term again represents the effect of the change of the absorption band due to thermalization. The population numbers for the different states satisfy the following rate equations:

$$\frac{dn_1}{dt} = -\frac{n_1}{T_1} \tag{5}$$

$$\frac{dn^*_0}{dt} = \frac{n_1}{T_1} - \frac{n^*_0}{\tau_{eq}} \tag{6}$$

$$\frac{dn_0}{dt} = \frac{n^*_0}{\tau_{eq}} \tag{7}$$

$$N = n_0 + n_1 + n^*_0 \tag{8}$$

The rate equations can be solved leading to

$$n_1(t) = n_1(0)\,e^{-t/T_1} \tag{9}$$

$$n_0{}^*(t) = \frac{1}{T_1/\tau_{eq} - 1}\left(e^{-t/T_1} - e^{-t/\tau_{eq}}\right)n_1(0) + e^{-t/\tau_{eq}}n_0(0) \tag{10}$$

$$n_0(t) = N - n_1(t) - n^*_0(t) \tag{11}$$

These functions are convolved with the measured cross correlation function of the pump and probe beam to account for the finite spectral width of our pulses. This gives us the full expressions for $-\Delta\alpha_{01}(\omega,t)$ and $\Delta\alpha_{12}(\omega,t)$ which can be compared to the measured $\ln(T/T_0)$. Fitting these functions to the actual data gives us the time constants T_1 and τ_{eq}, as well as the ratio $\sigma^*_{01}/\sigma_{01}$ at the probe frequency.

The curves resulting from the fit are depicted in Figure 2 for water. Due to the overwhelming contribution of the thermalization effect in water the measurements shown in Figures 2a−c are not very sensitive to the value of T_1 of the first relaxation process. The contribution of the thermalization is somewhat less pronounced in Figure 2d. Hence we used this measurement to determine the value of T_1 by fitting eq 4. This results in a value of T_1 of 130 ± 40 fs. For τ_{eq} we find $\tau_{eq} = 850 \pm 50$ fs. We have used the value for T_1 as a constant in eq 2 in the other fits. The resulting equilibration times are τ_{eq} 560 ± 30, 500 ± 30, and 590 ± 30 fs for probing at 3280, 3410, and 3500 cm^{-1}, respectively.

In the case of ethanol, the same procedure is followed. Fitting of Figure 4d with eq 4 yields $T_1 = 400 \pm 60$ fs and $\tau_{eq} = 2.1 \pm 0.1$ ps. For the probe wavelengths 3265, 3310, and 3450 cm^{-1} (Figure 4c, b, and a, respectively), we find $\tau_{eq} = 8 \pm 1$, 13.5 ± 2.0, and 3.0 ± 0.3 ps by fitting eq 2. For methanol we observe an equilibration time of 1.1 ± 0.1 ps and a T_1 of 220 ± 40 fs when probing at 3150 cm^{-1} and an equilibration time τ_{eq} of 7.2 ± 0.5 ps when probing at 3330 cm^{-1} (results not shown). For 1-propanol the equilibration time is 3.0 ± 0.2

ps and T_1 is 380 ± 60 fs when probing at 3150 cm^{-1}, and τ_{eq} is 15 ± 5 ps when probing at 3330 cm^{-1}(results not shown).

V. Discussion

In our experiment the response of the OH-stretch vibration is used to monitor the equilibration process. This OH-stretch vibration is very sensitive to changes in the relative positions of the water and alcohol molecules. The observed blue shift of the OH-stretch absorption band and the decrease of the cross-section thus directly reflect the repositioning of the molecules that follows from the dissipation of energy. It should be noted that the equilibration involves two subsequent processes. The first process is formed by the energy redistribution in which the energy of the nonthermal intermediate level becomes thermally distributed over all degrees of freedom. After this redistribution the equilibration is not yet complete because putting energy in a particular degree of freedom does not imply that the coordinate corresponding to this degree of freedom instantaneously finds its new equilibrium position. For instance, if a molecule is excited with a short pulse to a dissociative potential, it still takes some time, determined by the time scale of the nuclear motion, before the molecule is really dissociated. In a similar fashion it takes some time after the energy has been redistributed before the low-frequency translational and rotational degrees of freedom have acquired their new equilibrium positions. Hence, after the first process of energy redistribution, the equilibration involves a second process in which the molecules attain their new equilibrium positions. This repositioning of the molecules is directly observed in our experiment.

The question arises whether the energy redistribution or the repositioning forms the rate-limiting step of the overall equilibration. It can be expected that the three-dimensional hydrogen-bonded network of water allows for a much faster redistribution of energy than the one-dimensional hydrogen-bonded chains[22−24] of methanol, ethanol, and propanol. Hence, if the energy redistribution would form the rate-limiting step of the equilibration, water is expected to show a faster equilibration than the three alcohols, as indeed is observed. However, in that case the three alcohols are expected to have very similar equilibration times, which is certainly not the case. If, on the other hand, the repositioning of the molecules forms the rate-limiting step of the equilibration, the equilibration rate is expected to scale inversely with the mass of the molecules. This agrees quite well with the observation that the equilibration time constant increases going from water to methanol, ethanol, and propanol. If the overall equilibration time is indeed determined by the rate of the repositioning of the molecules, the time scales of the equilibration of water, methanol, ethanol, and propanol should correlate with those observed in dielectric relaxation and rotational correlation experiments.

Dielectric relaxation measurements[25,26] on the pure liquids show Debye relaxation times of about 8 ps for water, 50 ps for methanol, about 160 ps for pure ethanol, and about 320 ps for 1-propanol. Rotational correlation times for OH-groups obtained by NMR spectroscopy yield 2.6 ps for water,[27] 5 ps for methanol,[28] 18 ps for ethanol,[28] and 33 ps for propanol.[28] Hence, dielectric relaxation and NMR measurements show a very similar increase in time constant going from water to methanol to ethanol to 1-propanol as is observed for the equilibration. This strongly suggests that at least for the alcohols the repositioning of the molecules forms the rate-limiting step in the equilibration. However, for the fastest liquid, being liquid water, the rate of equilibration could still be limited by the rate of energy redistribution.

It should be noted that, although the trend matches, the absolute values of the Debye relaxation time, the rotational correlation time, and the equilibration time do not match exactly. Here it should be realized that although reorientation, as it is measured in Debye relaxation and rotational correlation experiments, and thermalization are not the same processes. The repositioning of the molecules in a thermalization process mainly involves a change of the distance between the molecules, e.g., the hydrogen-bond lengths. Recently, the hydrogen-bond dynamics has been studied for liquid water.[29,30] The correlation time constant of the hydrogen-bond length was observed to be approximately 500 fs. From the comparison of this time scale with the rotational correlation time constant of approximately 2.6 ps, it is clear that the modulation of the hydrogen-bond length is a faster process than the reorientation of the molecules. Hence, it is not surprising that the time scales measured for the equilibration process are shorter than the Debye relaxation and rotational correlation time constants.

A striking difference between the equilibration of the alcohols and liquid water is the frequency dependence of the equilibration time. For the alcohols the equilibration time constant strongly depends on the probe frequency, in the wings of the OH-stretch absorption band the equilibration time constant is much shorter than in the center of the absorption band. In contrast, for water the equilibration time constant is practically the same at all frequencies. A closer look at the fits to the alcohol data also shows that the equilibration process is not truly singly exponential, in the early stages the equilibration is somewhat faster than the fitted exponential function and at longer times the equilibration is somewhat slower than the fitted function.

The frequency dependence of the fitted equilibration time constant and the nonexponential character of the equilibration of the alcohols indicates that at least two time scales are involved in the equilibration process of the alcohols, i.e., in the repositioning of the molecules. It should be realized that shifts of the absorption spectrum will much more affect the transmission measured in the wings of the absorption than in the center, whereas a decrease in the absorption cross-section will have a similar effect on all probe frequencies. The fact that the fitted equilibration time constant is much shorter in the wings (Figures 4a,d) than in the center (Figures 4b,c) thus indicates that the blue shift of the absorption band occurs on a shorter time scale than the decrease of the absorption cross-section. This difference in time scale indicates that the shift of the absorption band and the decrease in cross-section are associated with the dynamics in *different* degrees in freedom.

The total picture is now as follows. After the energy has been redistributed over all degrees of freedom, the coordinates of the low-frequency modes should find their new equilibrium positions. For the low-frequency modes that determine the frequency of the OH-stretch vibration this repositioning is a faster process than for the low-frequency modes that determine the cross-section of the OH-stretch vibration. A low-frequency mode that strongly affects the OH-stretch frequency is the hydrogen-bond stretching vibration. With increasing length of the hydrogen bond, the OH-stretch frequency shifts to higher values. A low-frequency mode that will strongly influence the absorption cross-section of the OH-stretch vibration is the hydrogen-bond bending mode. A change in the hydrogen-bond bending coordinate can decrease the amount in which the OH-groups on different alcohol molecules are in line. Thereby the conjugation of the OH-stretch vibrations is reduced which leads to a decrease of the absorption cross-section. The characteristic frequency of the hydrogen-bond bending mode is much lower than that of the hydrogen-bond stretching mode. For instance, for water the frequencies of the hydrogen-bond bending and stretching modes are approximately 50 cm^{-1} and 200 cm^{-1}, respectively.[31] The fact that the frequency is lower also means that it will take a longer time before the new equilibrium position is attained. Hence, the difference in time scale observed for the shift of the absorption and the decrease in absorption cross-section are likely due to the fact that these changes correspond to the dynamics in the hydrogen-bond stretch and the hydrogen-bond bending mode, respectively.

For water the equilibration time hardly depends on the probe frequency which strongly suggests that for water the rate of equilibration is not limited by the rate at which the water molecules attain their new positions in the liquid but rather by the rate of energy redistribution. Hence for water the observed equilibration time constant is mainly determined by the relaxation rate of the nonthermal intermediate state. This means that the observed time scale of ~0.55 ps just presents an upper limit for the time scale on which the molecules in liquid water reposition following a dissipation of energy.

VI. Conclusions

Using two-color femtosecond mid-infrared pump−probe spectroscopy, we investigated the equilibration dynamics of water, methanol, ethanol, and 1-propanol, following a local deposition of energy. In the experiments, the OH-stretch vibration is excited that relaxes to a nonthermal intermediate state, which is formed by specific combination tone(s) of excited intra- and intermolecular vibrations. The relaxation of this nonthermal intermediate state leads to a complete (thermal) equilibration of the energy. The dynamics of the latter equilibration process is monitored via the spectral response of the OH-stretch vibration. We observe that the equilibration leads to a blue shift of the OH-stretch absorption band and a decrease of the absorption cross section. Using a kinetic modeling of the experimental data we find that the time constants of equilibration of water, methanol, ethanol, and 1-propanol are 0.55−0.85, 1.1−7.2, 2.1−13, and 3.0−15 ps, respectively. The equilibration time scale increases with increasing molecular mass, which indicates that for the alcohols the rate of equilibration is determined by the rate at which the molecules can change their relative orientations and positions in the liquid.

For the alcohols the frequency dependence of the equilibration time constant suggests that the blue shift of the absorption band is much faster than the decrease in absorption cross-section. A likely explanation for this observation is that the blue-shift results from the motion in the hydrogen-bond stretch coordinate and the decrease in cross-section results from the slower motion in the hydrogen-bond bending coordinate.

For water, we observe a very short equilibration time constant of 0.55 ps, which, in contrast to the alcohols, hardly depends on frequency. This suggests that for water the equilibration rate is not determined by the repositioning of the molecules (as for the alcohols) but rather by the rate of energy relaxation from a nonthermal intermediate state. Hence, the reposition of the molecules in liquid water probably occurs on a time scale that is shorter than 0.55 ps. This means that water can adapt extremely fast, much faster than alcohols, to a deposition of energy.

Acknowledgment. We thank L.D. Noordam for fruitful discussions. The research presented in this paper is part of the research program of the Foundation for Fundamental Research on Matter (FOM) and was made possible by financial support of The Netherlands Organization for Scientific Research (NWO).

References and Notes

(1) Jimenez, R.; Fleming, G. R.; Kumar, P. V.; Maroncelli, M. *Nature* **1994**, *369*, 471.

(2) Pant, P.; Riter, R. E.; Levinger, N. E. *J. Chem. Phys.* **1998**, *109*, 9995.

(3) Novak, A. *Struct. Bonding* (Berlin) **1974**, *18*, 177.

(4) Hadži, D.; Bratos, S. In *The Hydrogen Bond*; Schuster, P., Zundel, G., Sandorfy, C., Eds.; Elsevier: Amsterdam, 1976; Vol. 2, Chapter 12.

(5) Pettitt, B. M.; Karplus, M. *Chem. Phys. Lett*. **1987**, *136*, 383.

(6) Cui, Q.; Karplus, M. *J. Chem. Phys*. **2000**, *112*, 1133.

(7) Whitnell, R. M.; Wilson, K. R.; Hynes, J. T. *J. Chem. Phys.* **1992**, *96*, 5354.

(8) Rey, R.; Hynes, J. T. *J. Chem. Phys*. **1996**, *104*, 2356.

(9) Mountain, R. *J. Chem. Phys*. **1995**, *103*, 3084.

(10) Vodopyanov, K. L. *Sov. Phys. JETP* **1982**, *55*, 1049.

(11) Vodopyanov, K. L. *Sov. Phys. JETP* **1986**, *64*, 67.

(12) Vodopyanov, K. L. *Sov. Phys. JETP* **1990**, *70*, 114.

(13) Vodopyanov, K. L. *J. Chem. Phys*. **1991**, *94*, 5389.

(14) Woutersen, S.; Emmerichs, U.; Nienhuys, H.-K.; Bakker, H. J. *Phys. Rev. Lett.* **1998**, *81*, 1106.

(15) Emmerichs, U.; Woutersen, S.; Bakker, H. J. *J. Opt. Soc. Am. B* **1997**, *14*, 1478.

(16) Graener, H.; Seifert, G.; Laubereau, A. *Chem. Phys. Lett*. **1990**, *172*, 435.

(17) Graener, H.; Seifert, G.; Laubereau, A. *Phys. Rev. Lett.* **1991**, *66*, 2092.

(18) Palfrey, S. L.; Heinz, T. F. *J. Opt. Soc. Am. B* **1985**, *2*, 674.

(19) Finzi, J., et al. *J. Chem. Phys.* **1977**, *67*, 4053.

(20) Deak, J. C.; Rhea, S. T.; Iwaki, L. K.; Dlott, D. D. *J. Phys. Chem. A* **2000**, *104*, 4866.

(21) Nienhuys, H.-K.; Woutersen, S.; Van Santen, R. A.; Bakker, H. J. *J. Chem. Phys*. **1999**, *111*, 1494.

(22) Saiz, L.; Padro, J. A.; Guardia, E. *J. Phys. Chem. B* **1997**, *101*, 78.

(23) Laenen, R.; Rauscher, C. *J. Chem. Phys*. **1997**, *107*, 9759.

(24) Jorgensen, W. L. *J. Phys. Chem*. **1986**, *90*, 1276.

(25) Barthel, J.; Bachhuber, K.; Buchner, R.; Hetzenauer, H. *Chem. Phys. Lett*. **1990**, *165*, 369.

(26) Kindt, J. T.; Schmuttenmaer, C. A. *J. Phys. Chem*. **1996**, *100*, 10373.

(27) Smith, D. W. G.; Powles, J. G. *Mol. Phys*. **1966**, *10*, 451.

(28) Ludwig, R.; Zeidler, M. D. *Mol. Phys*. **1994**, *82*, 313.

(29) Gale, G. M.; Gallot, G.; Hache, F.; Lascoux, N.; Bratos, S.; Leicknam, J.-C. *Phys. Rev. Lett*. **1999**, *82*, 1086.

(30) Woutersen, S.; Bakker, H. J. *Phys. Rev. Lett*. **1999**, *83*, 2077.

(31) Walrafen, G. E. *J. Chem. Phys*. **1990**, *94*, 2237.